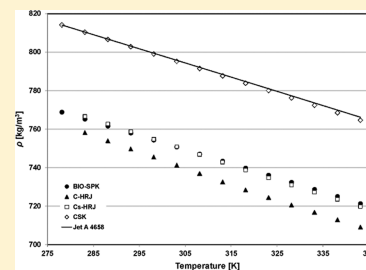


Density and Speed of Sound Measurements of Four Bioderived Aviation Fuels

Stephanie L. Outcalt* and Tara J. Fortin

Material Measurement Laboratory, Applied Chemicals and Materials Division, National Institute of Standards and Technology, 325 Broadway, Boulder, Colorado 80305-3337, United States

ABSTRACT: Compressed-liquid densities and ambient-pressure densities and speeds of sound of four biomass-derived fuels have been measured. The compressed-liquid measurements were made from (270 to 470) K and (0.5 to 50) MPa. The ambient-pressure measurements were made from (278 to 343) K. Compressed-liquid density data at 10 MPa and below were extrapolated to 0.083 MPa and, in combination with the ambient-pressure data, fitted to a Rackett equation, to allow comparison of the two sources of data. Additionally, the compressed-liquid density data have been correlated to a Tait equation, and parameters are given for each fuel.



1. INTRODUCTION

In recent years, the need to secure supply chains and escalating fuel costs has resulted in an increased interest in substitute aviation fuels that are derived from nonpetroleum feed stock. Sources of potential feed stocks include plants and animals, and each potential feed stock has a number of unique factors that contribute to the viability of its use. For example, for plant sources, the ease with which a crop is grown, including the amount of water it requires and the amount of land needed to yield a given amount of feed stock, is an initial consideration.¹ If the economics of obtaining the feed stock are determined to be reasonable, the complexity of the process through which the fuel is ultimately derived must then be considered. If that is also considered favorable, it then makes sense to study the thermophysical properties of the fuel to determine whether it can be used efficiently as an alternative to aviation kerosene.

The data reported here are part of a larger project to characterize aviation fuels derived from a variety of biomass feed stocks.^{1–3} Four fuels were studied in this work. Each fuel was derived from a different feed stock: camelina (a genus within the flowering plant family Brassicaceae⁴), castor seed (from the flowering plant *Ricinus communis*⁵), plant isoprenoid (derived from a fermentation process of sugar with a recombinant host cell⁶), and reclaimed waste fats and grease. Additional background information on each of the fuels is provided elsewhere.¹

Density (ρ) and speed of sound (ω) measurements were made for each of the four fuels and tabulated results are given. These measurements provide data necessary to formulate equations of state. By predicting fluid properties, these equations facilitate the optimization of potential new fuels as both direct substitutes, and as additives to traditional aviation kerosene that help extend the supply and/or enhance the performance. For engineering and design purposes, adiabatic compressibilities have been derived from the ambient-pressure density and speed of sound data and are also reported. Compressed-liquid density data have been extrapolated to 0.083 MPa and combined with ambient-pressure density data to correlate a Rackett equation for density.

Additionally, compressed-liquid densities have been correlated with a Tait equation. Parameters for all of the correlations are reported. Finally, as the fuels are being considered primarily for aviation, the ambient-pressure density and speed of sound data reported here have been compared to a previously measured petroleum based Jet A sample.⁷ The Jet A sample chosen for comparison, designated Jet A-4658 (also known as POSF 4658), is generically representative of the typical range of properties exhibited within the specifications for Jet A. The Jet A-4658 sample was prepared at the Air Force Research Laboratory by combining five separate, orthogonal batches of Jet A.

2. SAMPLE LIQUIDS

The samples measured in this work were provided by the Propulsion Directorate of the Air Force Research laboratory at Wright Patterson Air Force Base in Ohio and were from the same allotment as those reported in Bruno and Baibourine¹ and Bruno et al.² Extensive distillation curve data and chemical analysis of the four fuel samples were reported in those works; thus only general information will be provided here. The Air Force designated the samples of camelina, plant isoprenoid, and waste fat and grease as POSF 6152, POSF 5630, and POSF 5469 respectively; however, to maintain continuity between the reports of Bruno and Baibourine,¹ Bruno et al.,² and this work, each of the four fuel samples will be referred to in this work by the same acronym used in those previous publications. The acronyms are as follow: camelina (C-HRJ), castor seed oil (CS-HRJ), plant isoprenoid (CSK), and waste fat and grease (BIO-SPK). The work of Bruno and Baibourine¹ documents that although the primary constituents of both the C-HRJ and the CS-HRJ samples were found to be linear and branched paraffins, the

Received: July 20, 2012

Accepted: August 26, 2012

Published: September 13, 2012

Table 1. Measured Densities and Speeds of Sound and Derived Adiabatic Bulk Modulus for the Four Biomass-Derived Fuels at 0.083 MPa

<i>T</i>	BIO-SPK			C-HRJ		
	ρ	<i>w</i>	κ_s	ρ	<i>w</i>	κ_s
K	kg·m ⁻³	m·s ⁻¹	TPa ⁻¹	kg·m ⁻³	m·s ⁻¹	TPa ⁻¹
278.15	768.83 ± 0.06	1349.3 ± 1.5	714.4			
283.15	765.20 ± 0.06	1328.5 ± 1.5	740.4	758.20 ± 1.09	1302.3 ± 0.4	777.7
288.15	761.58 ± 0.06	1308.0 ± 1.4	767.5	753.97 ± 1.22	1281.8 ± 0.4	807.2
293.15	757.95 ± 0.06	1287.7 ± 1.4	795.7	749.70 ± 1.16	1261.7 ± 0.5	837.9
298.15	754.31 ± 0.06	1267.8 ± 1.3	824.8	745.52 ± 1.28	1241.8 ± 0.5	869.9
303.15	750.68 ± 0.06	1248.2 ± 1.3	855.1	741.33 ± 1.21	1222.1 ± 0.5	903.2
308.15	747.03 ± 0.06	1228.8 ± 1.3	886.6	736.90 ± 1.15	1202.5 ± 0.5	938.5
313.15	743.38 ± 0.06	1209.6 ± 1.3	919.4	732.62 ± 0.92	1183.2 ± 0.6	975.0
318.15	739.72 ± 0.06	1190.7 ± 1.3	953.6	728.39 ± 0.44	1164.2 ± 0.7	1013.0
323.15	736.05 ± 0.06	1171.9 ± 1.3	989.2	724.39 ± 0.22	1145.3 ± 0.9	1052.4
328.15	732.37 ± 0.06	1153.4 ± 1.3	1026.4	720.57 ± 0.20	1126.7 ± 1.3	1093.3
333.15	728.68 ± 0.06	1135.0 ± 1.3	1065.2	716.76 ± 0.20	1108.2 ± 1.6	1136.1
338.15	724.99 ± 0.06	1116.9 ± 1.3	1105.7	712.94 ± 0.20	1089.8 ± 2.1	1181.1
343.15	721.27 ± 0.06	1099.0 ± 1.3	1147.9	709.09 ± 0.20	1071.3 ± 1.8	1228.9

<i>T</i>	Cs-HRJ			CSK		
	ρ	<i>w</i>	κ_s	ρ	<i>w</i>	κ_s
K	kg·m ⁻³	m·s ⁻¹	TPa ⁻¹	kg·m ⁻³	m·s ⁻¹	TPa ⁻¹
278.15				814.14 ± 0.10	1357.5 ± 0.4	666.6
283.15	766.58 ± 0.41	1323.8 ± 0.5	744.4	810.37 ± 0.10	1336.9 ± 0.4	690.4
288.15	762.66 ± 0.29	1303.7 ± 0.5	771.5	806.60 ± 0.09	1316.8 ± 0.4	715.0
293.15	758.70 ± 0.25	1283.9 ± 0.4	799.5	802.83 ± 0.09	1296.6 ± 0.4	740.9
298.15	754.77 ± 0.32	1264.2 ± 0.4	829.0	799.05 ± 0.09	1276.8 ± 0.4	767.7
303.15	750.86 ± 0.41	1244.9 ± 0.4	859.4	795.27 ± 0.09	1257.1 ± 0.4	795.7
308.15	746.83 ± 0.55	1225.5 ± 0.4	891.5	791.48 ± 0.09	1237.6 ± 0.4	824.9
313.15	742.83 ± 0.60	1206.5 ± 0.4	924.8	787.68 ± 0.09	1218.3 ± 0.4	855.3
318.15	738.76 ± 0.45	1187.7 ± 0.4	959.6	783.86 ± 0.09	1199.1 ± 0.4	887.2
323.15	734.74 ± 0.18	1169.0 ± 0.5	996.0	780.04 ± 0.09	1180.1 ± 0.4	920.5
328.15	730.96 ± 0.18	1150.4 ± 0.5	1033.8	776.21 ± 0.09	1161.2 ± 0.4	955.4
333.15	727.25 ± 0.18	1132.0 ± 0.5	1073.1	772.36 ± 0.09	1142.5 ± 0.4	991.9
338.15	723.51 ± 0.18	1113.7 ± 0.6	1114.3	768.50 ± 0.09	1123.9 ± 0.4	1030.2
343.15	719.76 ± 0.18	1095.7 ± 0.6	1157.3	764.61 ± 0.09	1105.6 ± 0.4	1069.9

distillation curve of the Cs-HRJ is approximately 20 °C below that of C-HRJ from beginning to end. This indicates that although the two samples have several components in common, their relative contributions to the overall composition are very different, resulting in the observed differences in the distillation curves. The CSK sample is composed predominantly of closely boiling cyclic compounds, resulting in a distillation curve that is essentially flat at approximately 171 °C. The distillation curve of the BIO-SPK has an initial boiling temperature and an end temperature similar to those of the Cs-HRJ sample, but the shape of the curve is more linear than that of Cs-HRJ. The composition of the BIO-SPK sample² includes many constituents similar to the C-HRJ and the Cs-HRJ samples; however, all of the constituents are present at gas chromatographic peak area percentages between 1.5 and 3.3. In contrast, the composition analysis of the C-HRJ, Cs-HRJ, and CSK samples^{1,8,9} had area percent ranges of 2.2 to 10.7, 1.0 to 7.9, and 4.3 to 47.1, respectively. The small range of area percentages in the BIO-SPK sample indicates that there are no clearly dominant components in the fuel, and this probably contributes to the linear nature of the distillation curve.

Ambient-pressure density and sound speed measurements were carried out using the samples as they were received.

However, prior to the compressed-liquid density measurements, the samples were transferred to stainless steel cylinders and degassed by freezing the sample with liquid nitrogen and evacuating the vapor space. After evacuation, the sample was then heated (in the closed stainless steel cylinder) to drive any remaining dissolved impurities into the vapor space. The cooling and evacuation were then repeated, and the entire cycle (cooling, evacuation, and heating) was repeated a minimum of three times for each sample.

3. EXPERIMENTAL SECTION

A commercial density and sound speed analyzer was used to measure both properties at ambient-pressure (approximately 0.083 MPa). Details of the instrument and experimental procedures can be found in Laesecke et al.¹⁰ and Fortin et al.;¹¹ thus, only a brief description will be given here. The instrument contains two measurement cells in series; a sound speed cell that measures the propagation time of approximately 3 MHz sound waves and a vibrating-tube densimeter constructed of borosilicate glass. Temperature is measured with an integrated Pt-100 thermometer with an estimated uncertainty of 0.03 K. The instrument was calibrated with deionized water and toluene over the entire temperature range. During measurements, temperature scans were performed

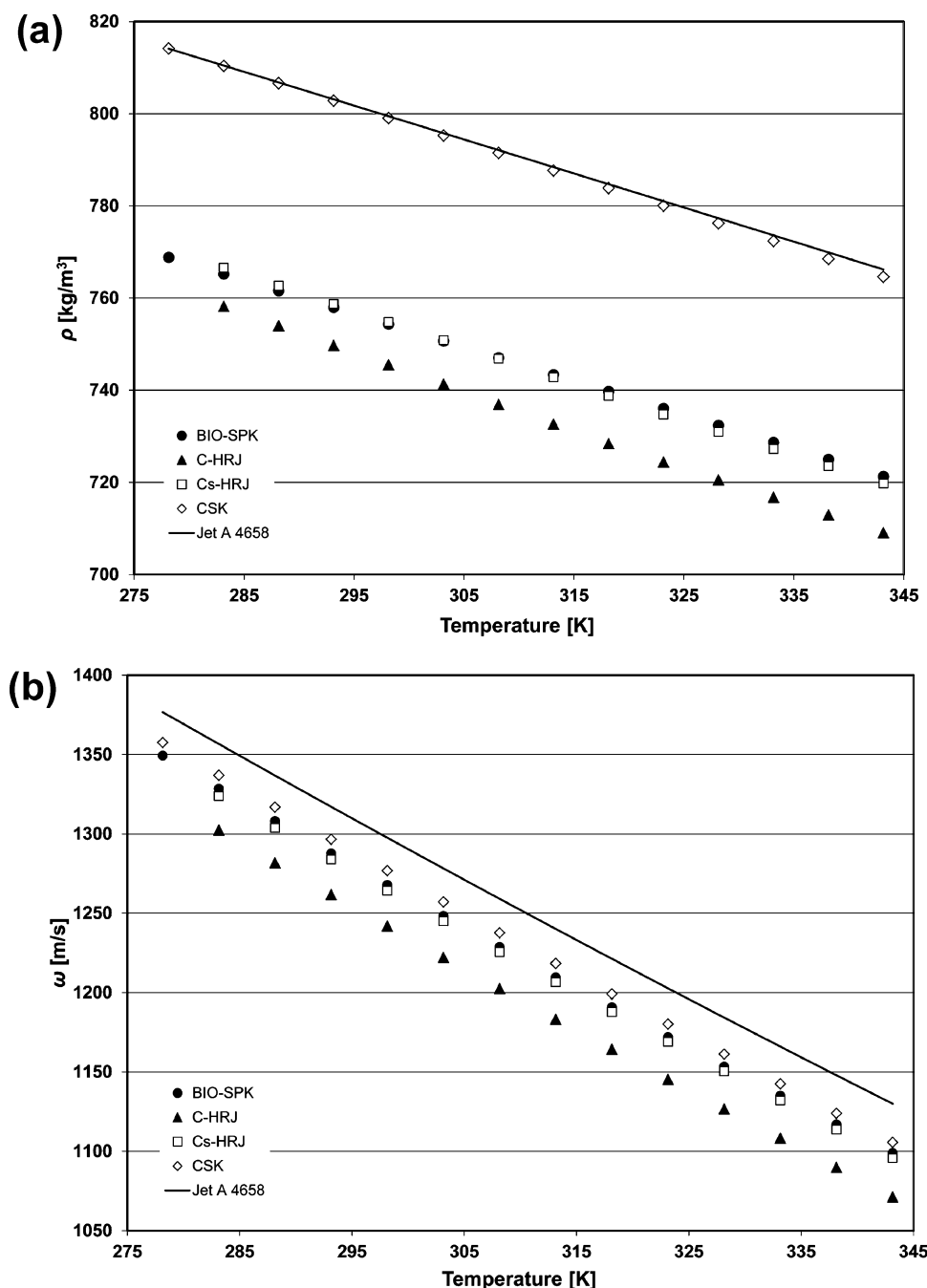


Figure 1. (a) Measured densities of the biomass-derived fuels and of Jet A 4658 as a function of temperature at 0.083 MPa. (b) Measured speeds of sound of the biomass-derived fuels and of Jet A 4658 as a function of temperature at 0.083 MPa.

from (343 to 278) K in decrements of 5 K. A fresh sample of fuel was injected for each temperature scan rather than performing repetitive measurements on the same sample. At least three temperature scans were performed for each fuel. For the ambient-pressure density and sound speed measurements, the uncertainties (95% confidence level) are listed with the reported data (Table 1).

The densities of the compressed test liquids were measured with the automated densimeter of Outcalt and McLinden.¹² Central to the apparatus is a commercial vibrating-tube densimeter. Several physical and procedural improvements have been implemented to minimize the uncertainty in the measurements. Some of these

improvements include more accurate measurements of temperature and pressure, better temperature control, and complete automation of the instrument control and data acquisition. The temperature range of the instrument is (270 to 470) K, with pressures up to 50 MPa. The instrument was calibrated with propane and toluene over the entire temperature and pressure range. Further details of the calibration procedure can be found in Outcalt and McLinden.¹² The overall combined uncertainty ($k = 2$, 95% confidence level) in density is $0.81 \text{ kg}\cdot\text{m}^{-3}$, corresponding to a relative uncertainty in density of 0.1% to 0.13%. In this work, we measured eleven isotherms over the range (0.5 to 50) MPa for each of the fuel samples.

Table 2. Compressed-Liquid Densities of BIO-SPK Measured in the High-Pressure Vibrating-Tube Densimeter^a

270 K		290 K		310 K		330 K		350 K		370 K	
<i>p</i>	ρ	<i>p</i>	ρ	<i>p</i>	ρ	<i>p</i>	ρ	<i>p</i>	ρ	<i>p</i>	ρ
MPa	kg·m ⁻³	MPa	kg·m ⁻³	MPa	kg·m ⁻³	MPa	kg·m ⁻³	MPa	kg·m ⁻³	MPa	kg·m ⁻³
50.04	801.9	49.99	790.3	50.00	778.7	49.99	767.1	50.03	755.6	50.02	744.3
40.01	797.2	40.00	785.2	40.01	773.1	40.00	761.2	40.00	749.2	40.01	737.4
30.00	792.1	30.00	779.7	30.01	767.1	30.00	754.8	30.00	742.3	30.00	730.0
20.01	786.8	20.00	773.9	20.00	760.7	20.01	747.8	20.00	734.7	20.01	721.7
10.01	781.1	10.01	767.6	10.01	753.8	10.01	740.1	10.00	726.2	10.01	712.4
5.00	778.1	5.01	764.2	5.00	750.0	5.00	736.0	5.00	721.6	5.01	707.2
4.01	777.4	4.00	763.5	4.01	749.3	4.01	735.1	4.01	720.6	4.00	706.1
3.01	776.8	3.01	762.8	3.01	748.5	3.00	734.2	3.00	719.7	3.01	705.0
2.00	776.2	2.00	762.1	2.01	747.7	2.01	733.3	2.01	718.7	2.01	703.8
1.00	775.5	1.00	761.4	1.01	746.9	1.01	732.4	1.00	717.6	1.01	702.7
0.51	775.2	0.51	761.0	0.50	746.5	0.51	732.0	0.50	717.1	0.50	702.1
0.083	775.0	0.083	760.7	0.083	746.1	0.083	731.6	0.083	716.6	0.083	701.6
390 K		410 K		430 K		450 K		470 K			
<i>p</i>	ρ	<i>p</i>	ρ	<i>p</i>	ρ	<i>p</i>	ρ	<i>p</i>	ρ		
MPa	kg·m ⁻³	MPa	kg·m ⁻³	MPa	kg·m ⁻³	MPa	kg·m ⁻³	MPa	kg·m ⁻³		
50.00	733.3	50.03	722.3	50.01	711.3	50.00	700.6	50.02	690.1		
40.01	725.9	40.00	714.4	40.00	702.8	40.01	691.6	40.00	680.4		
30.00	717.8	30.00	705.6	30.00	693.4	30.00	681.3	30.00	669.3		
20.00	708.8	20.00	695.7	20.01	682.6	20.00	669.5	20.01	656.4		
10.01	698.5	10.01	684.2	10.00	669.8	10.01	655.3	10.00	640.6		
5.00	692.7	5.00	677.6	5.00	662.4	5.01	646.9	5.00	631.0		
4.01	691.4	4.01	676.3	3.99	660.8	4.00	645.1	4.01	628.9		
3.01	690.1	3.00	674.8	3.00	659.1	3.00	643.2	3.01	626.7		
2.01	688.8	2.00	673.3	2.00	657.5	2.01	641.3	2.01	624.4		
1.00	687.5	1.01	671.9	1.00	655.7	1.01	639.2	1.00	622.0		
0.50	686.9	0.50	671.1	0.50	654.8	0.51	638.2	0.50	620.8		
0.083	686.3	0.083	670.5	0.083	654.1	0.083	637.3	0.083	619.8		

^aValues extrapolated to 0.083 MPa are indicated in italics. The combined expanded uncertainties U_c are $U_c(T) = 30$ mK, $U_c(p) = 0.01$ MPa, $U_c(\rho) = 0.81$ kg·m⁻³ (level of confidence = 0.95).

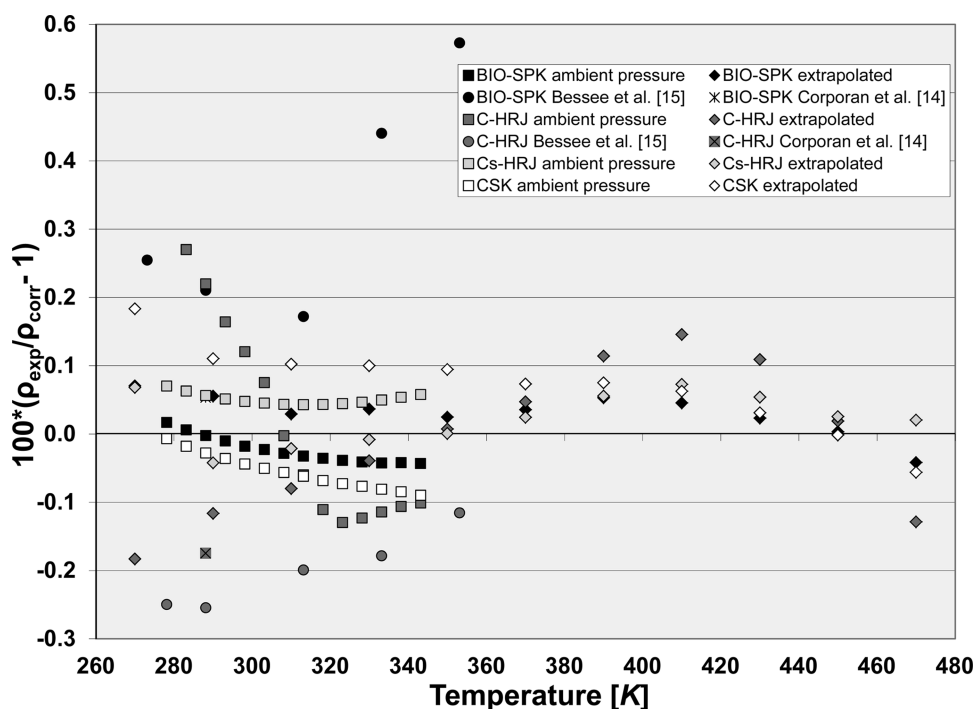


Figure 2. Deviations of measured and extrapolated ambient-pressure density data of the BIO-SPK, C-HRJ, Cs-HRJ, and CSK samples from their respective Rackett correlations.

Table 3. Compressed-Liquid Densities of Camelina C-HRJ Measured in the High-Pressure Vibrating-Tube Densimeter^a

270 K		290 K		310 K		330 K		350 K		370 K	
<i>p</i>	ρ	<i>p</i>	ρ	<i>p</i>	ρ	<i>p</i>	ρ	<i>p</i>	ρ	<i>p</i>	ρ
MPa	kg·m ⁻³	MPa	kg·m ⁻³	MPa	kg·m ⁻³	MPa	kg·m ⁻³	MPa	kg·m ⁻³	MPa	kg·m ⁻³
49.99	792.7	49.99	780.6	49.98	768.8	50.00	756.7	50.01	745.2	50.00	733.8
39.99	787.8	39.99	775.4	39.99	763.1	39.99	750.6	39.99	738.6	40.00	726.6
30.00	782.7	29.99	769.7	29.99	756.9	29.99	743.9	29.99	731.4	30.00	718.9
20.00	777.1	19.99	763.7	20.00	750.2	20.00	736.7	19.99	723.5	19.99	710.2
9.99	771.2	9.99	757.1	10.00	743.0	9.99	728.7	9.99	714.6	10.00	700.4
5.00	768.1	5.00	753.6	4.99	739.0	4.99	724.3	4.99	709.7	4.99	694.9
3.99	767.4	3.99	752.9	3.99	738.2	4.00	723.4	3.99	708.7	3.99	693.8
2.99	766.8	2.99	752.2	3.00	737.4	2.99	722.5	3.00	707.7	2.99	692.6
1.99	766.1	1.99	751.4	1.99	736.5	1.99	721.6	1.99	706.6	1.99	691.4
0.99	765.5	0.99	750.7	0.99	735.7	0.99	720.6	0.99	705.5	0.99	690.2
0.49	765.1	0.49	750.3	0.49	735.3	0.50	720.1	0.49	705.0	0.49	689.6
0.083	764.9	0.083	750.0	0.083	734.9	0.083	719.7	0.083	704.5	0.083	689.1
390 K		410 K		430 K		450 K		470 K			
<i>p</i>	ρ	<i>p</i>	ρ	<i>p</i>	ρ	<i>p</i>	ρ	<i>p</i>	ρ		
MPa	kg·m ⁻³	MPa	kg·m ⁻³	MPa	kg·m ⁻³	MPa	kg·m ⁻³	MPa	kg·m ⁻³		
50.01	722.7	50.00	711.9	50.00	701.2	50.00	690.7	50.01	680.5		
39.98	715.1	39.99	703.8	39.99	692.5	39.99	681.3	39.99	670.5		
29.98	706.7	29.99	694.7	29.99	682.7	29.98	670.7	29.99	659.0		
19.99	697.3	19.99	684.4	19.99	671.4	19.99	658.4	20.00	645.5		
9.99	686.5	9.99	672.4	10.00	658.0	9.99	643.5	9.99	628.8		
4.99	680.3	4.99	665.5	4.99	650.1	4.99	634.4	4.99	618.4		
4.00	679.0	3.99	664.0	3.99	648.4	4.00	632.5	4.00	616.1		
2.99	677.7	2.99	662.5	2.99	646.7	2.99	630.5	2.99	613.8		
1.99	676.4	1.99	660.9	2.00	644.9	2.00	628.4	1.99	611.3		
1.00	675.0	0.99	659.4	0.99	643.1	0.99	626.2	1.00	608.7		
0.49	674.3	0.49	658.6	0.49	642.2	0.49	625.1	0.49	607.4		
0.083	673.7	0.083	657.9	0.083	641.4	0.083	624.2	0.083	606.3		

^aValues extrapolated to 0.083 MPa are indicated in italics. The combined expanded uncertainties U_c are $U_c(T) = 30$ mK, $U_c(p) = 0.01$ MPa, $U_c(\rho) = 0.81$ kg·m⁻³ (level of confidence = 0.95).

4. RESULTS

Table 1 lists values of density, speed of sound, and derived adiabatic compressibilities for the four biomass-derived samples at ambient-pressure from (278.15 to 343.15) K. Adiabatic compressibilities (κ_s) were calculated from the measured densities and speeds of sound via the thermodynamic relation

$$\kappa_s = 1/(\rho w^2) \quad (1)$$

where ρ is the density and w is the speed of sound. The adiabatic bulk modulus can be obtained by calculating the inverse of the reported adiabatic compressibilities. The ambient-pressure density and speed of sound data are depicted graphically in Figure 1a,b, respectively. For comparison, previously measured density and sound speed values⁷ for a conventional petroleum-based jet fuel, Jet A-4658, are also shown. Figure 1a shows that the densities for BIO-SPK and Cs-HRJ are relatively similar. In contrast, density values for C-HRJ are lower than those of other fuel samples, whereas those of CSK are substantially larger and very similar to those of Jet A-4658. Figure 1b illustrates that the speeds of sound of the four biomass-derived fuels all fall below those of Jet A 4658 and that, like the density values, the values for BIO-SPK and Cs-HRJ are very similar.

Listed in Tables 2–5 are measured values of compressed-liquid density from (270 to 470) K at pressures to 50 MPa for BIO-SPK, C-HRJ, Cs-HRJ, and CSK, respectively. Also listed are density values extrapolated to 0.083 MPa (this is the approximate

atmospheric pressure in Boulder, CO) for each temperature. These were obtained by fitting a second-order polynomial to the isothermal data at pressures less than or equal to 10 MPa and extrapolating to 0.083 MPa. This was done to examine the consistency of the compressed-liquid data with the measurement results at ambient-pressure from the density and sound speed analyzer.

5. CORRELATION OF DATA

The density measurements at ambient-pressure and values extrapolated to 0.083 MPa from measured compressed-liquid data presented in this work were correlated with a Rackett-type equation¹³ to facilitate the comparison of our two data sets and existing literature data. The equation is written as

$$\rho = \beta_1 \cdot \beta_2^{-(1+(1-T/\beta_3)^{\beta_4})} \quad (2)$$

The resulting correlation parameters for each of the four fuels are listed in Table 6. In Figure 2, the correlations serve as the baseline to compare the ambient-pressure and extrapolated values for BIO-SPK, C-HRJ, Cs-HRJ, and CSK. It can be seen that our measured and extrapolated data for the BIO-SPK and Cs-HRJ samples agree within their stated uncertainties. There is agreement (within experimental uncertainties) between our two data sets at temperatures above 290 K for the C-HRJ, but the agreement between the CSK data sets is just outside the bounds of their uncertainties. No Cs-HRJ or CSK ambient-pressure

Table 4. Compressed-Liquid Densities of Cs-HRJ Measured in the High-Pressure Vibrating-Tube Densimeter^a

270 K		290 K		310 K		330 K		350 K		370 K	
<i>p</i>	ρ	<i>p</i>	ρ	<i>p</i>	ρ	<i>p</i>	ρ	<i>p</i>	ρ	<i>p</i>	ρ
MPa	kg·m ⁻³	MPa	kg·m ⁻³	MPa	kg·m ⁻³	MPa	kg·m ⁻³	MPa	kg·m ⁻³	MPa	kg·m ⁻³
50.02	801.8	49.99	789.3	50.04	777.7	49.97	766.2	50.00	754.9	50.03	743.6
40.00	797.0	39.99	784.08	40.00	772.2	40.00	760.2	39.99	748.5	39.99	736.7
29.99	791.9	30.00	778.55	29.99	766.2	29.99	753.8	29.99	741.5	30.00	729.2
19.99	786.6	19.99	772.67	19.99	759.8	19.99	746.8	19.99	733.9	19.99	720.8
9.99	780.8	9.99	766.33	10.00	752.9	9.99	739.1	9.99	725.4	9.99	711.4
4.99	777.7	4.99	762.95	4.99	749.1	4.98	734.9	4.99	720.7	4.98	706.2
3.99	777.1	4.01	762.27	4.00	748.3	3.99	734.1	4.00	719.7	3.99	705.1
2.99	776.5	2.99	761.55	2.99	747.5	2.99	733.2	3.00	718.7	2.99	704.0
2.00	775.8	1.99	760.84	1.99	746.7	1.99	732.3	1.99	717.7	2.00	702.8
0.99	775.2	0.99	760.12	0.99	745.9	0.99	731.4	0.99	716.7	0.99	701.7
0.49	774.9	0.49	759.76	0.49	745.5	0.49	730.9	0.49	716.2	0.49	701.1
0.083	774.6	0.083	759.5	0.083	745.2	0.083	730.6	0.083	715.7	0.083	700.6
390 K		410 K		430 K		450 K		470 K			
<i>p</i>	ρ	<i>p</i>	ρ	<i>p</i>	ρ	<i>p</i>	ρ	<i>p</i>	ρ		
MPa	kg·m ⁻³	MPa	kg·m ⁻³	MPa	kg·m ⁻³	MPa	kg·m ⁻³	MPa	kg·m ⁻³		
49.98	732.5	50.03	721.5	49.99	710.4	50.01	699.5	50.01	688.8		
40.00	725.1	40.00	713.5	40.00	701.8	40.00	690.3	40.00	679.1		
29.99	717.0	29.99	704.7	29.99	692.3	30.00	680.0	29.99	667.9		
19.99	707.9	19.99	694.8	19.99	681.4	19.99	668.1	20.00	654.9		
10.00	697.5	10.00	683.2	10.00	668.5	9.99	653.8	9.99	638.9		
4.99	691.6	4.99	676.6	4.99	661.0	4.99	645.2	4.99	629.2		
4.00	690.3	3.99	675.2	3.99	659.4	3.99	643.4	3.99	627.0		
2.99	689.1	2.99	673.7	2.99	657.7	2.99	641.4	3.00	624.8		
1.99	687.7	1.99	672.2	1.99	656.0	1.99	639.5	1.99	622.4		
1.00	686.4	1.00	670.7	0.99	654.3	1.00	637.4	0.99	620.0		
0.50	685.8	0.49	669.9	0.49	653.4	0.49	636.3	0.49	618.8		
0.083	685.2	0.083	669.3	0.083	652.7	0.083	635.5	0.083	617.8		

^aValues extrapolated to 0.083 MPa are indicated in italics. The combined expanded uncertainties U_c are $U_c(T) = 30$ mK, $U_c(p) = 0.01$ MPa, $U_c(\rho) = 0.81$ kg·m⁻³ (level of confidence = 0.95).

density data were found in the literature. Two sources of such data were found for samples of BIO-SPK and C-HRJ.^{14,15} The samples studied in refs 14 and 15 were from the same batches as samples used in this work. Those data are included in Figure 2 but were not used in the correlations. The data of Corporan et al.¹⁴ (one point at 288.15 K for each sample) agree well with our extrapolated data. The C-HRJ ambient-pressure density data of Bessee et al.¹⁵ agree with our extrapolated data within experimental uncertainty, but for BIO-SPK that is not the case. The BIO-SPK data of Bessee et al.¹⁵ are consistently higher than either of our data sets.

To make the present results immediately usable for engineering and design purposes, the compressed-liquid density data were correlated with a Tait equation similar to that of Dymond and Malhotra.¹⁶ The temperature dependence of the parameter C was omitted because it was not needed to fit the majority of the data within their experimental uncertainty. The equation used to fit the compressed-liquid density data is

$$\rho(T, p) = \frac{\rho_{\text{ref}}(T, p_{\text{ref}})}{1 - C \ln\left(\frac{p + B(T)}{p_{\text{ref}} + B(T)}\right)} \quad (3)$$

where $\rho_{\text{ref}}(T)$ is the temperature-dependent density at the reference pressure p_{ref} (0.083 MPa); $p_{\text{ref}}(T)$ was calculated with eq 2. The temperature dependence of the Tait parameter $B(T)$ was expressed by a quadratic polynomial,

$$B(T) = \beta_5 + \beta_6 T_r + \beta_7 T_r^2 \quad (4)$$

where T_r is the absolute temperature T divided by 273.15 K. The resulting parameters for the Tait correlations for all four fuels are given in Table 7. Panels a–d of Figure 3 show deviations of the measured compressed-liquid density data from baselines that represent the Tait correlations for BIO-SPK, C-HRJ, Cs-HRJ, and CSK, respectively. As shown in Figure 3a–d, the Tait correlations successfully represent the majority of our data within their stated uncertainty. The only exceptions are eight points for C-HRJ and six points for CSK along their respective 270 K isotherms, and a single point for C-HRJ along the 470 K isotherm.

6. CONCLUSIONS

Density and speed of sound at ambient-pressure and compressed-liquid densities of four biomass-derived fuel samples, BIO-SPK, C-HRJ, Cs-HRJ, and CSK, have been measured covering a combined temperature range of (270 to 470) K with pressures to 50 MPa. The compressed-liquid density data have been correlated with a modified Tait equation that fits the majority of the measured data within their experimental uncertainty.

Knowledge of the composition and distillation curve of each fuel may aid in understanding and interpreting the data. For example, the very similar distillation curves of the BIO-SPK and Cs-HRJ may indicate that both samples contain many of the

Table 5. Compressed-Liquid Densities of CSK Measured in the High-Pressure Vibrating-Tube Densimeter^a

270 K		290 K		310 K		330 K		350 K		370 K	
<i>p</i>	ρ	<i>p</i>	ρ	<i>p</i>	ρ	<i>p</i>	ρ	<i>p</i>	ρ	<i>p</i>	ρ
MPa	kg·m ⁻³	MPa	kg·m ⁻³	MPa	kg·m ⁻³	MPa	kg·m ⁻³	MPa	kg·m ⁻³	MPa	kg·m ⁻³
49.99	849.1	49.98	836.4	50.01	824.2	49.97	812.1	50.01	800.1	50.05	788.1
40.00	844.3	40.01	831.2	40.00	818.6	40.01	806.0	40.00	793.5	40.00	781.0
30.00	839.1	30.00	825.6	30.01	812.5	30.01	799.5	30.01	786.5	30.00	773.4
20.00	833.7	20.01	819.7	20.00	806.0	20.01	792.5	20.01	778.8	20.00	765.0
10.00	827.9	10.00	813.3	10.00	799.0	10.00	784.7	10.00	770.3	10.01	755.6
5.01	824.8	5.00	809.9	5.00	795.3	5.00	780.6	5.00	765.6	5.01	750.4
4.00	824.2	4.01	809.2	4.01	794.5	4.00	779.7	4.00	764.7	4.00	749.3
3.01	823.6	3.01	808.5	3.01	793.7	3.00	778.8	3.01	763.7	3.00	748.2
2.00	822.9	2.00	807.7	2.00	792.9	1.99	777.9	2.00	762.7	2.00	747.1
0.99	822.3	1.00	807.0	1.01	792.1	1.01	777.0	1.00	761.7	1.00	745.9
0.50	822.0	0.50	806.7	0.50	791.7	0.50	776.6	0.51	761.2	0.50	745.3
0.083	821.7	0.083	806.3	0.083	791.3	0.083	776.2	0.083	760.7	0.083	744.8
390 K		410 K		430 K		450 K		470 K			
<i>p</i>	ρ	<i>p</i>	ρ	<i>p</i>	ρ	<i>p</i>	ρ	<i>p</i>	ρ		
MPa	kg·m ⁻³	MPa	kg·m ⁻³	MPa	kg·m ⁻³	MPa	kg·m ⁻³	MPa	kg·m ⁻³		
50.00	776.3	50.01	764.8	49.95	753.2	50.00	742.0	49.97	730.9		
40.00	768.8	40.01	756.7	40.01	744.6	39.99	732.7	40.00	721.0		
30.00	760.6	30.00	747.8	30.00	734.9	30.01	722.2	30.00	709.6		
20.00	751.4	20.01	737.8	20.00	723.9	20.00	710.1	20.00	696.3		
10.00	741.0	10.01	726.1	10.01	710.9	10.01	695.6	10.00	680.1		
5.00	735.1	5.00	719.5	5.01	703.4	5.02	687.1	5.00	670.2		
4.00	733.9	4.00	718.1	4.00	701.8	4.00	685.2	4.01	668.0		
3.00	732.6	3.01	716.6	3.00	700.1	3.00	683.2	3.00	665.7		
2.01	731.3	2.00	715.1	2.00	698.4	2.00	681.3	2.01	663.4		
1.00	730.0	1.00	713.6	1.00	696.7	1.00	679.2	1.00	661.0		
0.50	729.3	0.50	712.9	0.51	695.8	0.50	678.2	0.51	659.7		
0.083	728.8	0.083	712.2	0.083	695.1	0.083	677.3	0.083	658.7		

^aValues extrapolated to 0.083 MPa are indicated in italics. The combined expanded uncertainties U_c are $U_c(T) = 30$ mK, $U_c(p) = 0.01$ MPa, $U_c(\rho) = 0.81$ kg·m⁻³ (level of confidence = 0.95).

Table 6. Rackett Correlation Parameters for the Density of Four Biomass-Derived Fuels Samples at Ambient-Pressure of 0.083 MPa and Temperatures from (270 to 470) K

parameter	BIO-SPK		C-HRJ	
	value	std dev	value	std dev
$\beta_1/\text{kg}\cdot\text{m}^{-3}$	127.7	0.4	238.6	0.4
β_2	0.3659	5.0×10^{-4}	0.4947	3.6×10^{-4}
β_3/K	642.7	0.2	577.2	0.3
β_4	0.4250	5.0×10^{-4}	0.6645	5.0×10^{-4}
parameter	Cs-HRJ		CSK	
	value	std dev	value	std dev
$\beta_1/\text{kg}\cdot\text{m}^{-3}$	146.2	0.2	216.3	0.3
β_2	0.3916	1.7×10^{-4}	0.4634	2.9×10^{-4}
β_3/K	622.32	0.08	595.1	0.2
β_4	0.4418	3.1×10^{-4}	0.5142	3.5×10^{-4}

same compounds and in relatively similar amounts. These similarities are observed in the ambient-pressure density and speed of sound as well as in the compressed-liquid densities, where the two fluids have almost equal values. In contrast, CSK has a distillation curve and composition significantly different from those of the other three biobased fuels, and also significantly larger densities. The differences between CSK and the other fuels are less pronounced in the sound speed data. Altogether, the data show the profound effect that composition has on the

Table 7. Tait Correlation Parameters for the Density of Four Biomass-Derived Fuels at Pressures to 50 MPa and Temperatures from (270 to 470) K

parameter	BIO-SPK		C-HRJ	
	value	std dev	value	std dev
<i>C</i>	0.08113	9×10^{-5}	0.08273	9×10^{-5}
β_5	304.4	0.5	363.3	0.5
β_6	-278.4	0.5	-361.0	0.5
β_7	65.8	0.2	93.5	0.2
parameter	Cs-HRJ		CSK	
	value	std dev	value	std dev
<i>C</i>	0.08003	9×10^{-5}	0.07803	9×10^{-5}
β_5	314.7	0.5	275.07	0.05
β_6	-293.3	0.5	-240.0	0.5
β_7	70.6	0.2	53.3	0.2

thermophysical properties of a fluid and how that effect is complicated by the complexity of these mixtures.

The four biomass-derived fuels studied in this work have densities and speeds of sound that are generally lower than those of a typical petroleum-based Jet A sample. The CSK (plant isoprenoid) sample exhibited properties most similar to those of Jet A and is the only sample of the four to meet the density specification (MIL-DTL-83133G)¹⁷ for military aviation fuels, which states that the fuel density at 288.15 K must be within (775

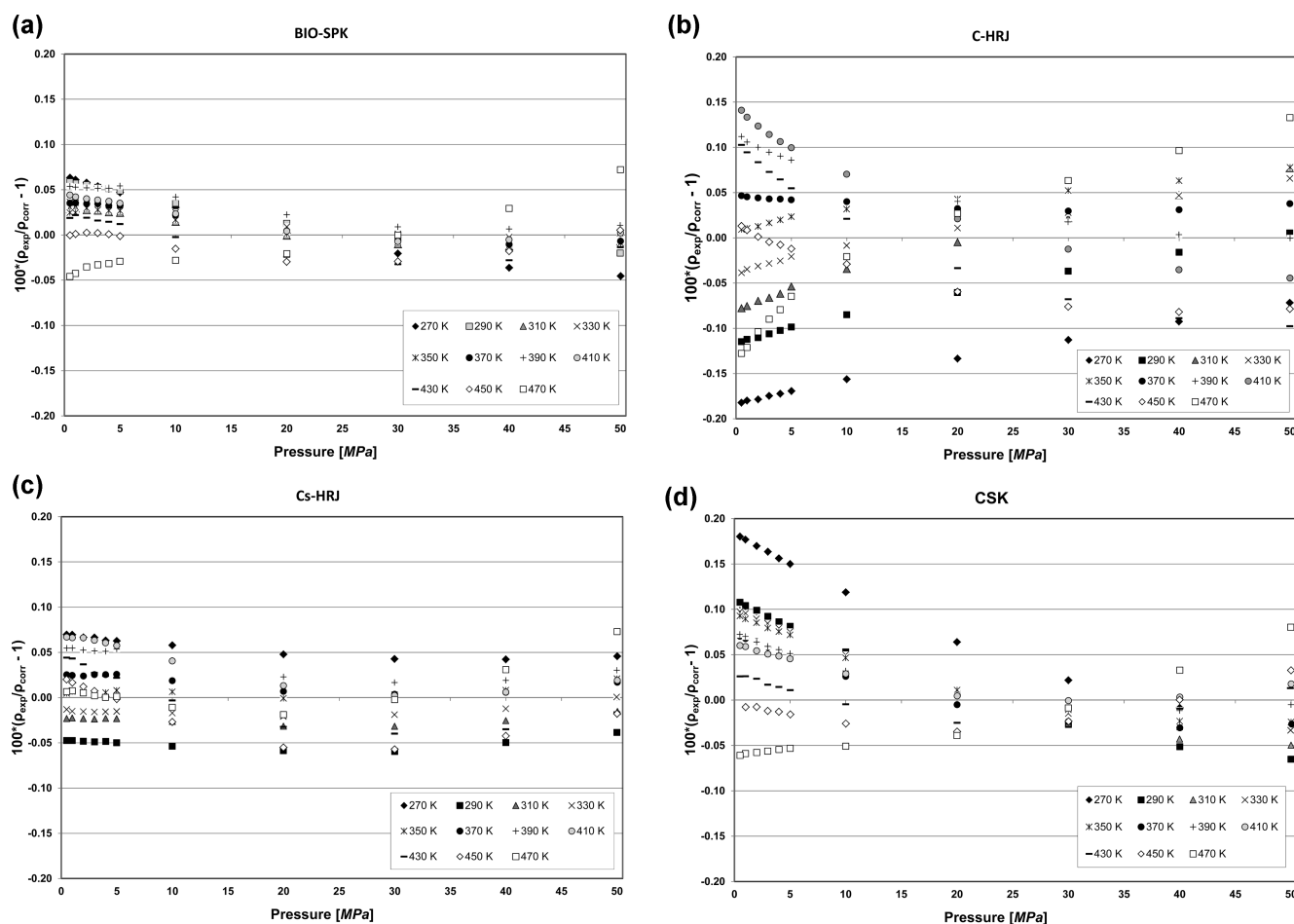


Figure 3. Deviations of compressed-liquid density data from the Tait correlation for (a) BIO-SPK, (b) C-HRJ, (c) Cs-HRJ, and (d) CSK.

and 840) $\text{kg}\cdot\text{m}^{-3}$. Thus the BIO-SPK, C-HRJ, and Cs-HRJ fuels are not adequate as stand-alone aviation fuel replacements under current specifications; however, as additives, they may have the potential to extend the supply and/or enhance the performance of other aviation fuels.

AUTHOR INFORMATION

Corresponding Author

*E-mail: Outcalt@Boulder.NIST.Gov.

Notes

The authors declare no competing financial interest.

ACKNOWLEDGMENTS

We thank the Propulsion Directorate of the Air Force Research laboratory at Wright Patterson Air Force Base in Ohio for providing the samples studied in this work.

REFERENCES

- (1) Bruno, T. J.; Baibourine, E. Comparison of Biomass-Derived Turbine Fuels with the Composition-Explicit Distillation Curve Method. *Energy Fuels* **2011**, *25*, 1847–1858.
- (2) Bruno, T. J.; Baibourine, E.; Lovestead, T. M. Comparison of Synthetic Isoparaffinic Kerosene Turbine Fuels with the Composition-Explicit Distillation Curve Method. *Energy Fuels* **2010**, *24*, 3049–3059.
- (3) Van Buren, J.; Abel, K.; Lovestead, T. M.; Bruno, T. J. Volatility of Mixtures of JP-8 with Biomass Derived Hydroprocessed Renewable Jet Fuels by the Composition Explicit Distillation Curve Method. *Energy Fuels* **2012**, *26*, 1964–1974.

- (4) Shonnard, D. R.; Williams, L.; Kalnes, T. N. Camilina-derived jet fuel and diesel: sustainable advanced biofuels, *Environ. Prog. Sustainable Energy*.

- (5) Brickell, C. *The American Horticultural Society Encyclopedia of Plants and Flowers*; American Horticultural Society Practical Guides; Cole, T., Cathey, H. M., Eds.; DK Adult Publishing: New York, NY, 2011; p 744.

- (6) Kirby, J.; Keasling, J. D. Biosynthesis of plant isoprenoids: perspectives for microbial engineering. *Annu. Rev. Plant Biol.* **2009**, *60*, 335–355.

- (7) Outcalt, S.; Laesecke, A.; Freund, M. B. Density and Speed of Sound Measurements of Jet A and S-8 Aviation Turbine Fuels. *Energy Fuels* **2009**, *23*, 1626–1633.

- (8) Bruno, T. J.; Svoronos, P. D. N. *CRC Handbook of Fundamental Spectroscopic Correlation Charts*; CRC Press: Boca Raton, FL, 2006.

- (9) Bruno, T. J.; Svoronos, P. D. N. *CRC Handbook of Basic Tables for Chemical Analysis*, 3rd ed.; CRC Press: Boca Raton, FL, 2011.

- (10) Laesecke, A.; Outcalt, S. L.; Brumback, K. J. Density and Speed of Sound Measurements of Methyl- and Propylcyclohexane. *Energy Fuels* **2008**, *22*, 2629–2636.

- (11) Fortin, T. J.; Laesecke, A.; Freund, M.; Outcalt, S. L. Advanced Calibration, Adjustment, and Operation of a Density and Sound Speed Analyzer. *J. Chem. Eng. Data* **2012**.

- (12) Outcalt, S. L.; McLinden, M. O. Automated Densimeter for the Rapid Characterization of Industrial Fluids. *Ind. Eng. Chem. Res.* **2007**, *46*, 8264–8269.

- (13) Rackett, H. G. Equation of State for Saturated Liquids. *J. Chem. Eng. Data* **1970**, *15*, 514.

- (14) Corporan, E.; Edwards, T.; Shafer, L.; DeWitt, M. J.; Klingshirn, C.; Zabarnick, S.; West, Z.; Striebich, R.; Graham, J.; Klein, J. Chemical, Thermal Stability, Seal Swell, and Emissions Studies of Alternative Jet Fuels. *Energy Fuels* **2011**, *25*, 955–966.

(15) Bessee, G. B.; Hutzler, S. A.; Wilson, G. R. *Propulsion and Power Rapid Response Research and Development (R&D) Support, Delivery Order 0011: Analysis of Synthetic Aviation Fuels*; Southwest Research Institute, USAF AFRL Technical Report, AFRL-RZ-WP-TR-2011-2084, April.

(16) Dymond, J. H.; Malhotra, R. The Tait equation: 100 years on. *Int. J. Thermophys.* **1988**, *9*, 941-951.

(17) NATO, *Detail Specification: Turbine Fuel, Aviation, Kerosene Type, JP-8 (NATO F-34), NATO F-35, and JP-8 + 100 (NATO F-37)*, MIL-DTL-83133G; Department of Defense, 30 April 2010.